applied sciences

MDPI

Article

Superior Photodegradation of Bentazon and Nile Blue and Their Binary Mixture Using Sol–Gel Synthesized TiO_2 Nanoparticles Under UV and Sunlight Sources

Sadaf Yasmeen [1], Luca Burratti [2,*], Leonardo Duranti [3], Emanuela Sgreccia [1], Antonio Agresti [4] and Paolo Prosposito [1,5]

[1] Industrial Engineering Department, University of Rome Tor Vergata, Via del Politecnico 1, 00133 Rome, Italy; sadaf.yasmeen@students.uniroma2.eu (S.Y.); emanuela.sgreccia@uniroma2.it (E.S.); paolo.prosposito@uniroma2.it (P.P.)
[2] Department of Engineering and Sciences, Mercatorum University, Piazza Mattei 10, 00186 Rome, Italy
[3] Department of Chemical Science and Technologies, University of Rome Tor Vergata, Via Della Ricerca Scientifica 1, 00133 Rome, Italy; leonardo.duranti@uniroma2.it
[4] Department of Electronic Engineering, University of Rome Tor Vergata, Via del Politecnico 1, 00133 Rome, Italy; antonio.agresti@uniroma2.it
[5] UdR INSTM of Rome Tor Vergata, 00133 Rome, Italy
* Correspondence: luca.burratti@uniroma2.it

Abstract: Herbicides and dyes in wastewater are considered serious water pollutants. These water pollutants have harmful effects on the ecosystem and due to this, the degradation of these pollutants is very important. In this article, titanium dioxide (TiO_2) nanoparticles were synthesized by the sol–gel method and used as photocatalysts. TiO_2 powder was characterized by using X-ray diffraction (XRD), scanning electron microscopy (SEM), Fourier-transform infrared spectroscopy (FTIR), and UV-Visible (UV-Vis) spectroscopy. The XRD analysis revealed the anatase phase for TiO_2. The SEM investigation showed that TiO_2 nanoparticles exhibit highly irregular block-shaped morphology. TiO_2 nanoparticles degrade the organic pollutants under UV as well as sunlight. The photocatalytic activity of such prepared catalyst was carried out in solutions of bentazon herbicide (BZ) and Nile blue dye (NB) and in the mixture of these pollutants, under UV and sunlight. The degradation rate of both BZ and NB was very high in individual solutions as well as in the combination of them. The obtained results show that TiO_2 photocatalyst is a potential candidate for the photocatalytic degradation of dyes and herbicides under UV and sunlight.

Keywords: TiO_2; sol–gel synthesis; photocatalysis; bentazon herbicide; Nile blue dye

Received: 7 January 2025
Revised: 31 January 2025
Accepted: 10 February 2025
Published: 12 February 2025

Citation: Yasmeen, S.; Burratti, L.; Duranti, L.; Sgreccia, E.; Agresti, A.; Prosposito, P. Superior Photodegradation of Bentazon and Nile Blue and Their Binary Mixture Using Sol–Gel Synthesized TiO_2 Nanoparticles Under UV and Sunlight Sources. *Appl. Sci.* **2025**, *15*, 1899. https://doi.org/10.3390/app15041899

1. Introduction

Water pollution is a worldwide problem and it has a dramatic impact on human health and aquatic life. In modern agriculture, the use of herbicides is intensively increasing to control the spread of weeds and protect crop growth [1]. Bentazon is a widely used herbicide, belongs to the thia-diazine group of chemicals, and it is specifically used in rice and soybean cultivations. At natural pH, bentazon high solubility and mobility in the soil contribute to pollution of surface and underground water [2].

Similarly, almost 80 million tons of dyes are produced annually worldwide and used in medical laboratories and industries such as textiles, paper, paint, food, and cosmetics. The release of a significant amount of these dyes into waterbodies disturbs the stability of ecosystems [3]. Nile blue dye is a potential photosensitizer that can be used in photodynamic

therapy to treat malignant tumors. Its release in the environment without any pretreatment is harmful to the respiratory tract if inhaled and causes skin and eye infections [4]. The discharge of polluted water with dyes and herbicides without any pretreatment represents a serious threat. Consequently, the development of cost-effective and eco-friendly methods for dye-containing water treatment is an urgent matter. Different biological, physical, and chemical methods have been used for the degradation of organic dyes and herbicides, such as reverse osmosis, coagulation, sedimentation, and the advanced oxidation process [5]. Notably, the advanced oxidation process (AOP) is a promising technique for the removal of organic pollutants (dyes and herbicides) by using semiconductor nanostructures due to the low cost, ecofriendly nature, high degradation efficiency, and chemical stability [6].

Metal oxide-based catalysts have been applied for the removal of organic pollutants including Fe_2O_3, ZnO, TiO_2, MgO, and Al_2O_3 [7–10]. Among these, titanium dioxide (TiO_2) has gained remarkable attention as a photocatalyst due to high photocatalytic activity towards organic pollutants, that can be combined to large surface area and adequate porosity. Titanium dioxide is the ninth most abundant chemical compound on the earth's crust, and it is present in three different phases: anatase, rutile, and brookite. Anatase TiO_2 is one of the stable crystalline phases of titania and has a high electron mobility and low recombination rate [11–13]. Owing to these properties, anatase TiO_2 is one of the most widely used photocatalysts for the light-driven degradation of organic pollutants. However, when TiO_2 nanoparticles were employed at the pilot scale, some disadvantages were encountered in the scaling up such as the cost, stability, and aggregation of TiO_2 nanoparticles, which may reduce the surface area and reduce the reactivity. In terms of toxicity, TiO_2 nanoparticles can pose health risks such as respiratory issues, skin irritation, and toxic effects on the aquatic system [14,15]. Numerous methods have been adopted for the fabrication of TiO_2 nanoparticles such as the co-precipitation method, hydrothermal synthesis, chemical vapor deposition, and sol–gel method. Among these, sol–gel is one of the most effective, low-cost, fast and feasible techniques to synthesize nanoparticles [16–18].

In this work, we prepared TiO_2 nanoparticles by the sol–gel method using $TiCl_4$ as a precursor. To investigate the physicochemical properties, the prepared TiO_2 photocatalyst was characterized by different characterization techniques such as X-ray diffraction (XRD), UV-Visible spectroscopy (UV-Vis), and Fourier-transform infrared spectroscopy (FTIR). Surface morphology was determined by scanning electron microscopy (SEM). In the present work, we used TiO_2 nanoparticles as a photocatalyst and studied the degradation efficiency towards single bentazon herbicide (BZ), Nile blue dye (NB), and herbicide and dye mixture (BZ + NB) under UV light and sunlight irradiation. To the best of our knowledge, this is the first work to report the high photocatalytic efficiency of TiO_2 towards such pollutants: with optimized conditions, 5 ppm contaminant concentration, pH 7, and catalyst loading of 20 mg, bentazon is 99% degraded in 40 min and Nile blue is degraded 100% in 160 min. The degradation of both pollutants in the BZ + NB mixture demonstrates that TiO_2 photocatalyst has the ability to degrade the pollutants simultaneously under UV and sunlight.

2. Materials and Methods

2.1. Chemicals

For the sample synthesis and photocatalytic experiments, all the chemicals were purchased from Merk (Darmstadt, Germany) and used as received. Titanium tetrachloride ($TiCl_4$) and absolute ethanol ($\geq$99.99%) were purchased and used as precursors. Nile blue ($C_{40}H_{40}N_6O_6S$, content $\geq$ 75%, powder) dye and bentazon ($C_{10}H_{12}N_2O_3S$, purity $\geq$ 98%, powder) herbicide were used as model organic pollutants.

2.2. Synthesis of TiO_2 Nanoparticles

For the synthesis of TiO_2 nanoparticles, the sol–gel method was used, as reported in the literature [19]. In a typical synthesis, 3.9 mL of $TiCl_4$ is taken and then slowly added to 10 mL of ethanol in a beaker at °C in an ice bath under a fume hood due to the exothermic reaction, release of hydrogen chloride, and high volatility of $TiCl_4$. After that, 0.5 mL of deionized water is added to the above mixture solution and the reaction is carried out under vigorous stirring. The mixture solution is then put in the oven at 80 °C for 18 h for drying. During the drying process, the mixture solution changes from colorless to yellow. The obtained TiO_2 powder is annealed for 2 h in a furnace at 600 °C temperature.

2.3. Photocatalytic Activity Experiment

The photocatalytic experiments were performed for the removal of Nile blue (NB) dye, bentazon herbicide (BZ), and their mixture (BZ + NB) under UV and sunlight irradiations. First, 20 mg of TiO_2 was mixed in 60 mL of model water (solution of NB, BZ, and solution of NB and BZ) with 5 ppm pollutant concentration. To attain the absorption/desorption equilibrium, polluted solutions in the presence of TiO_2 photocatalyst were placed in the dark and stirred for 1 h. Subsequently, the mixture solutions were exposed to irradiation of a UV lamp (300 W, Oriel Instruments, Newport, CA, USA) and natural sunlight. The intensity of the light was recorded during all the experiments by a power meter (Thorlabs, Newton, NJ, USA, model PM100D), finding a constant intensity of 126.5 mW/cm^2 and 2.58 mW/cm^2 for UV light and for sunlight, respectively. During the experiments, 3 mL of solution was taken after a consecutive time interval of 20 min and evaluated by using a double-beam UV-Vis spectrophotometer (Lambda 750, Perkin Elmer, Waltham, MA, USA). The degradation efficiency of the TiO_2 catalyst was calculated through Equation (1) [20].

$$Degradation\ efficiency = (C_0 - C_t)/C_0 \times 10 \quad (1)$$

2.4. Characterizations

The synthesized TiO_2 nanoparticles were characterized by using an X-ray diffractometer (Philips X-Pert Pro 500, Amsterdam, Nederland), with Cu Kα radiation (λ = 1.5418 Å) in the 20–80° 2θ range to determine the structure and calculate the crystal size and lattice parameters. The surface morphology was evaluated by the TESCAN MIRA FE-SEM instrument, where a secondary electron (SE) detector or an in-beam SE detector was employed to record the images, and the acceleration voltage at 5 kV and the probe current at 100 pA was set during the measurements. The optical properties of TiO_2 nanoparticles and photocatalytic measurements were investigated by a double-beam UV-Vis spectrophotometer. The Fourier-transform infrared spectrophotometer (Jasco FT/IR-4X, Victoria, BC, Canada) was used to evaluate the functional groups present in the sample.

3. Results and Discussions

3.1. X-Ray Diffraction

The X-ray diffraction was used to determine the crystal structure and phase purity of the prepared TiO_2 photocatalyst. Figure 1 shows the XRD spectra of the TiO_2 photocatalyst annealed at 600 °C. The obtained diffraction pattern was attributed to the anatase phase of TiO_2 and well matched with JCPDS (84-1286). The average crystallite size was calculated using the Scherrer equation $D = \frac{K\lambda}{\beta_{hkl}\ cos\ \theta}$ [21].

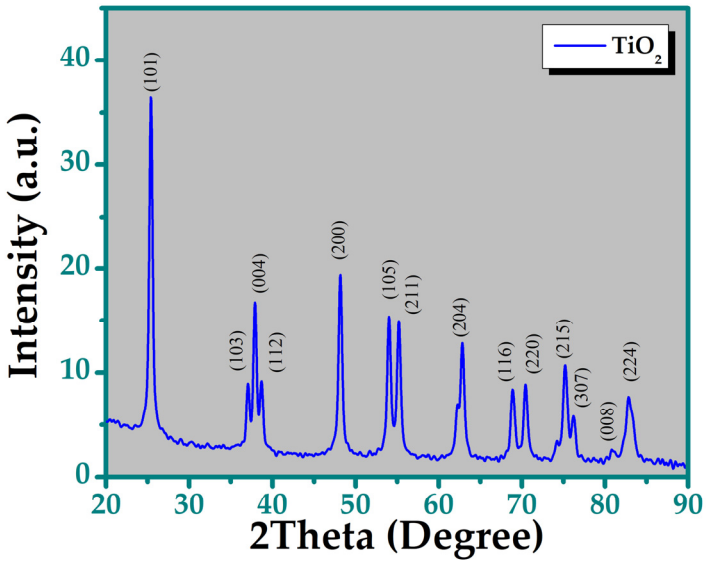

Figure 1. XRD spectra of prepared TiO_2 nanoparticles.

The calculated crystallite size and microstructural parameters [22] are listed in Table 1.

Table 1. Microstructural parameters of TiO_2 calculated from XRD pattern.

Parameters	TiO_2
Symmetry	Tetragonal Anatase
Lattice constants	a = 3.775 Å b = 9.581 Å
Cell volume	136.54 $Å^3$
Crystalline size D	20 nm

3.2. SEM Analysis

To determine the surface morphology and distribution of the prepared TiO_2 photocatalyst, scanning electron microscopy (SEM) images were collected at different magnifications as shown in Figure 2. The SEM images show that the TiO_2 photocatalyst exhibits a non-uniform distribution composed of irregularly shaped and agglomerated cubic structures.

3.3. FTIR

Figure 3a represents the FTIR spectra of the TiO_2 nanoparticles in the range of 450–4000 cm^{-1}. The band between 450 cm^{-1} and 800 cm^{-1} was attributed to Ti-O stretching and Ti-O-Ti bending vibrations. The band at 512 cm^{-1} and 721 cm^{-1} confirms the formation of the TiO_2 nanoparticles with the anatase phase [23]. The band located at 1209 cm^{-1} was assigned to the Ti-OH bending [24,25]. The strong band at 1740 cm^{-1} is due to the absorption of water molecules present in the atmosphere [26]. The weak band at 34,163 cm^{-1} as shown in Figure 3b corresponds to the hydroxyl groups (O-H) present on the surface of the TiO_2 catalyst which contribute to enhancing the photocatalytic activity [23].

3.4. UV-Visible Spectroscopy

The absorption spectra of TiO_2 nanoparticles were measured by using UV-Visible spectroscopy. Figure 4 displays the UV-Vis absorption spectra of the TiO_2 nanoparticles in the range of 200–800 nm. The optical band gap was calculated by the Tauc plot method using Equation (2) [27]:

$$\alpha h\upsilon = A\left(h\upsilon - E_g\right)^{1/2} \quad (2)$$

where h is Planck's constant, υ is the incident light frequency, A is a constant, and E_g represents the band gap energy, respectively. The band gap energy was calculated by plotting $(\alpha h\upsilon)^2$ vs. photon energy ($h\upsilon$) and extrapolating the value from the linear portion to $(\alpha h\upsilon)^2 = 0$ as shown in the inset of Figure 4. The calculated band gap of the TiO_2 photocatalyst was 3.12 eV [28].

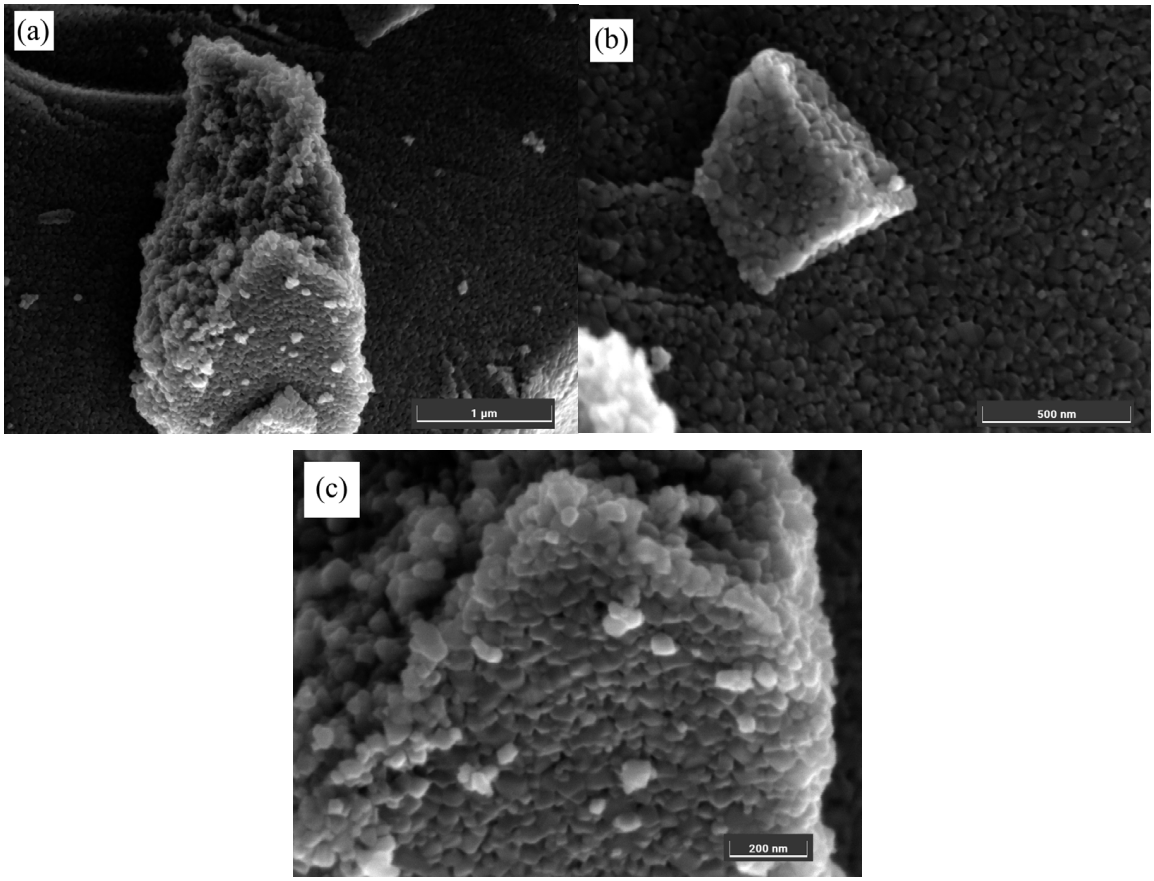

Figure 2. SEM images of prepared TiO_2 photocatalyst at different magnifications scale bars: (**a**) 1 µm, (**b**) 500 nm and (**c**) 200 nm.

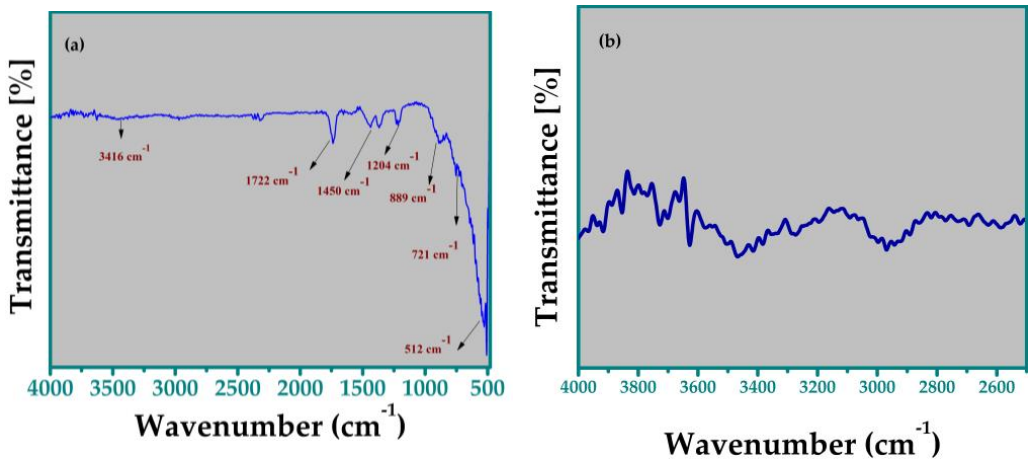

Figure 3. FTIR spectra of TiO_2 photocatalyst: (**a**) entire spectrum; (**b**) enlargement in the range of 2500–4000 cm^{-1}.

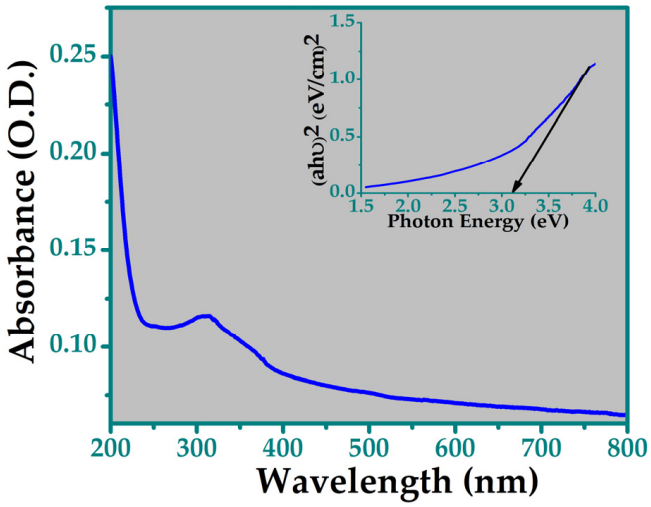

Figure 4. UV-Visible absorption spectra of the TiO_2 photocatalyst in the range of 200–800 nm. The inset shows the Tauc plot for the energy bandgap.

3.5. Photocatalytic Activity

The photocatalytic activity of the TiO_2 catalyst was investigated against the NB dye, BZ herbicide, and their solution under UV and natural sunlight irradiations. The change in pollutant concentration was recorded by acquiring the absorption spectra of the solution every 20 min.

3.5.1. Degradation of Bentazon Herbicide

The photodegradation of bentazon in the presence of 20 mg TiO_2 catalyst, 5 ppm pollutant concentration, and at pH 6, 7, 8, and 9 was carried out for 40 min under UV light. The obtained degradation efficiency was 81%, 99%, 43%, and 23% at pH 6, 7, 8, and 9, respectively, as shown in Figure 5a. The maximum degradation efficiency was obtained at pH = 7; thus, all photocatalytic experiments were performed at pH 7 under UV and sunlight irradiation.

Figure 5b,c shows the absorption spectra of BZ at different time intervals. The presence of a catalyst leads to a decrease in the absorption spectra at λ = 334 nm as a function of irradiation time, as shown in Figure 5a,b. The photocatalytic degradation efficiency of the TiO_2 catalyst against bentazon in 40 min was 99% and 75% under UV light and sunlight, respectively, as displayed in Figure 5d.

Additionally, the kinetic study of photodegradation was examined using a first-order model as follows [29]:

$$C_t = C_o e^{-kt} \quad (3)$$

$$ln\left(\frac{C_o}{C_t}\right) = kt \quad (4)$$

where k, C_o, and C_t represent the rate constant, and concentration of BZ before and after degradation under illumination as a function of time, respectively. The obtained results against the photodegradation of bentazon reveal that percentage degradation efficiency and rate constant k are higher under UV light as compared to sunlight. A literature comparison of the photocatalytic activity of TiO_2 for the degradation of bentazon at different experimental conditions is given in Table 2. The values of rate constants (k) and R^2 for BZ are listed in Table 3.

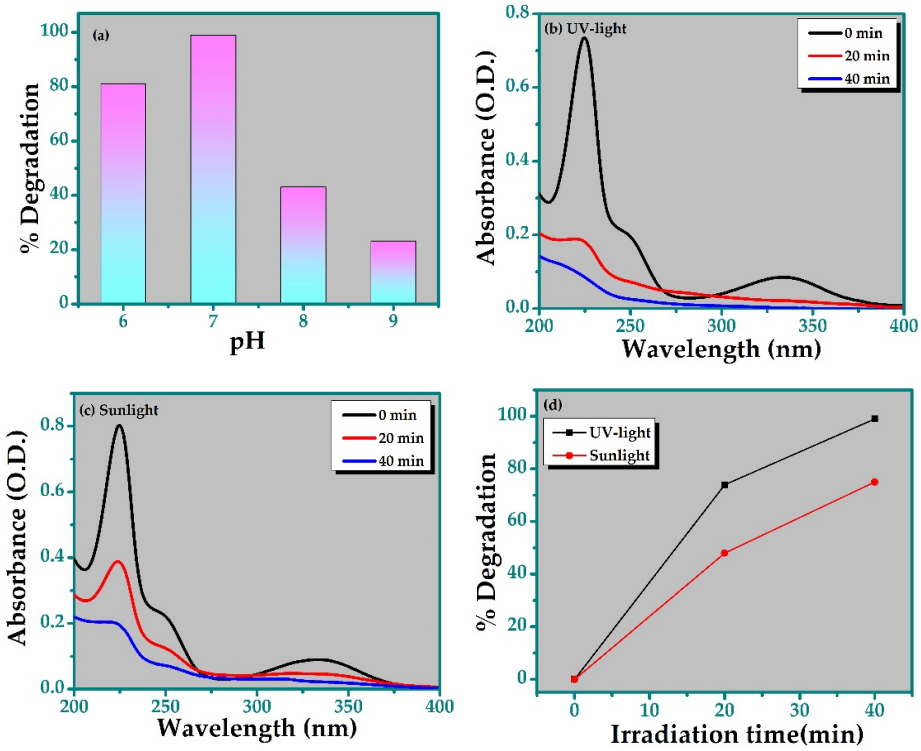

Figure 5. Degradation efficiency of BZ at different pH values (**a**); absorption spectra of BZ in the presence of the TiO_2 photocatalyst under UV (**b**) and sunlight (**c**); degradation efficiency at different irradiation times for the TiO_2 photocatalyst of BZ (**d**).

Table 2. The comparison study of photodegradation efficiency of TiO_2 and TiO_2-based composites at different experimental conditions for bentazon herbicide.

Catalyst	Catalyst Concentration (gL^{-1})	Irradiation Source	Bentazon Concentration (mgL^{-1})	% Degradation	Ref.
TiO_2 P25	1.0	Philips HB 175 60 W	20	85% in 120 min	[30]
TiO_2 nanocrystal	1.0	Philips HB 175 60 W	20	63% in 120 min	[30]
TiO_2 suspension	1.0	solar simulator 1000 W	10	95% in 60 min	[31]
TiO_2 suspension	1.0	sunlight	10	95% in 60 in	[31]
ZnO/TiO_2	0.5	UV lamp	20	80% in 120 min	[32]
TiO_2/PMAA	0.5	sunlight	10	100% in 200 min	[33]
TiO_2 nanoparticles	0.3	Hg lamp 300 W	5	99% in 40 min	Present work
-	-	sunlight	-	75% in 40 min	Present work

Table 3. Photodegradation kinetic parameters for TiO_2 catalyst against NB and BZ.

Pollutants	% Degradation	Radiation Source	K (min^{-1})	R^2	Y = a + bx
BZ	99%	UV	0.1110	0.9769	−0.2805 + 0.0110x
BZ	75%	sunlight	0.03491	0.9987	−0.0100 + 0.3491x
NB	98%	UV	0.0762	0.8859	−0.5997 + 0.0762x
NB	100%	sunlight	0.0355	0.8157	−0.8987 + 0.0355x
BZ (in BZ + NB mixture)	68%	UV	0.00679	0.9757	−0.0531 + 0.00679x
BZ (in BZ + NB mixture)	60%	Sunlight	0.0059	0.9575	−0.10543 + 0.0059x
NB (in BZ + NB mixture)	78%	UV	0.0093	0.9669	−0.1092 + 0.0093x
NB (in BZ + NB mixture)	95%	sunlight	0.0209	0.9289	−0.4136 + 0.0209x

3.5.2. Degradation of Nile Blue Dye

The photocatalytic activity of TiO_2 was also investigated against the Nile blue in the same experimental conditions as those used for bentazon, under UV and sunlight irradiations. The absorption spectra of NB in the presence of TiO_2 catalyst from 0 to 160 min are shown in Figure 6a,b under UV and natural sunlight irradiations, respectively.

Figure 6c shows the percentage degradation of NB dye. The percentage degradation of NB was 98% and 100% after 160 min under UV light and sunlight, respectively. Figure 6d represents the curve of $\ln(C/C_0)$ vs. time of irradiation. The values of rate constants (k) and R^2 for NB are listed in Table 3. The obtained results indicated that NB has a slightly higher percentage of degradation under sunlight as compared to UV light. A comparison of the TiO_2 photocatalytic activity against NB of our system with the other previous literature reports is given in Table 4.

Table 4. The comparison study of photodegradation efficiency of metal oxide-based nanocomposites at different experimental conditions for Nile blue.

Catalyst	Catalyst Concentration (gL^{-1})	Irradiation Source	Nile Blue Concentration (mgL^{-1})	Degradation Percentage	Ref.
$CuO\text{-}SiO_2$	0.1	UV lamp	20	90%	[34]
$FeMnO_3$	/	250 W mercury lamps	10	95% in 80 min	[35]
$CuFe_2O_4$	0.03	Hg lamp	10	93% in 120 min	[36]
NiO-ZnO	0.03	sunlight	5	97% in 140 min	[37]
TiO_2	0.3	UV light	5	98% in 160 min	Present work
TiO_2	0.3	Sunlight	5	100% in 160 min	Present work

3.5.3. Simultaneous Degradation of Bentazon and Nile Blue

The efficiency of TiO_2 was also assessed in a mixed solution of BZ and NB. The experiment was carried out in similar experimental conditions, both under UV and sunlight irradiation. Figure 7a,b shows the absorption spectra of the dye and herbicide mixture under UV and sunlight for 160 min. The absorption spectra show a simultaneous decrease at λ = 334 nm and λ = 634 nm for BZ and NB, respectively. Figure 7c shows the percentage degradation of BZ and NB in the mixture under the two irradiations. The percentage degradation of BZ and NB was 78% and 68% under UV light and 60% and 95% under sunlight. The degradation percentages are lower with respect to the single components for both organic pollutants. However, the removal percentage of BZ is lower as compared to NB under UV and sunlight. This might be due to the complex structure of NB which affects the degradation of BZ herbicide. $\ln(C_0/C_t)$ was plotted as a function of time (t) in Figure 7d. The values of rate constants (k) and R^2 are listed in Table 3. To the best of our knowledge, there are no experimental studies on the photocatalytic behavior of TiO_2 for the solution of BZ and NB under UV and sunlight. S. Prabhudesai et al. synthesized TiO_2 by the combustion method and used it for the degradation of individual solutions and a mixture of metamitron herbicide and rhodamine B dye. They observed the complete degradation of dye and herbicide under UV light [38]. Sabzehmeidani reported the degradation of two dyes Rhodamine B and methylene blue using ultrasound-assisted photocatalytic activity and obtained 63% and 97% degradation in the mixture solution [39].

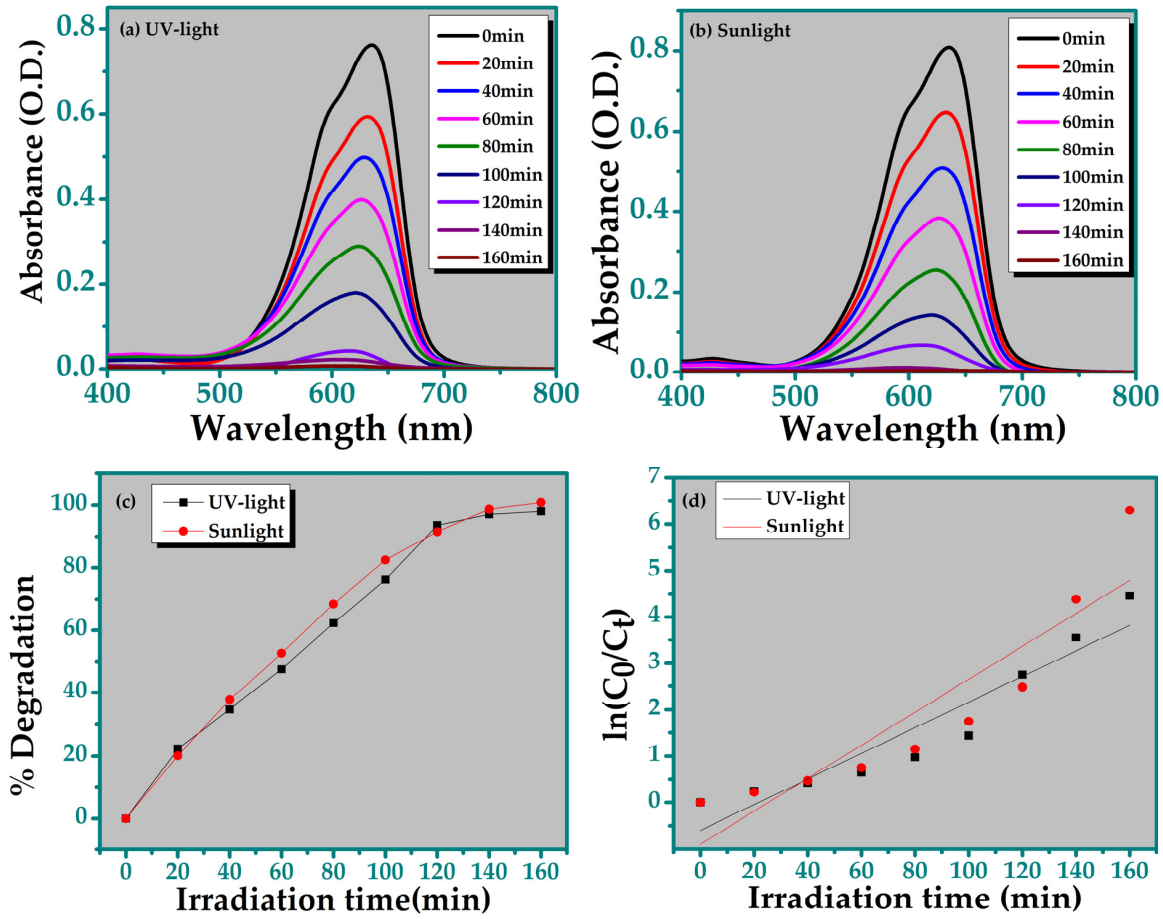

Figure 6. Absorption spectra of NB in the presence of the TiO_2 photocatalyst under UV (**a**) and sunlight (**b**); degradation efficiency at different time intervals (**c**); degradation rate constant plots (**d**).

3.5.4. Scavenger Test

To further confirm the photodegradation process and production of reactive species, the photodegradation process of bentazon was assessed by trapping experiment under UV light. 2-propanol and ascorbic acid were used as scavengers for hydroxyl radicals (*OH) and superoxide radicals ($\cdot O_2^-$). A dramatic decrease in the photodegradation efficiency was observed, which suggests the dominant role of the ROS species in the degradation of bentazon as shown in Figure 8. Without a scavenger, the obtained degradation efficiency of the TiO_2 catalyst was 99%. However, it is observed that the degradation efficiency is reduced from 99% to 27% and 13% in the presence of 2-propanol and ascorbic acid, respectively, which confirmed that the reactive species (*OH and $\cdot O_2^-$) are produced and have a dominant effect in the photodegradation of bentazon.

3.5.5. Stability and Reusability of TiO_2

To investigate the stability of TiO_2 photocatalyst, a reusability test was performed against bentazon under UV light at optimization conditions. After completing each cycle, the photocatalyst was collected by centrifuging (Thermo Fisher, Waltham, MA, USA, Megafuge 8), washed, and dried for 1 h at 70 °C. The obtained degradation efficiency of the TiO_2 for the three cycles is shown in Figure 9a. The structure and morphology of the catalyst after three cycles were investigated by means of XRD and SEM. The XRD peak profile before and after the reusability test is shown in Figure 9b, which confirms the structure stability of the TiO_2 photocatalyst. The SEM images of the reused catalyst also showed agglomerated cubic structures. There is no remarkable change after the reusability test as shown in Figure 9c.

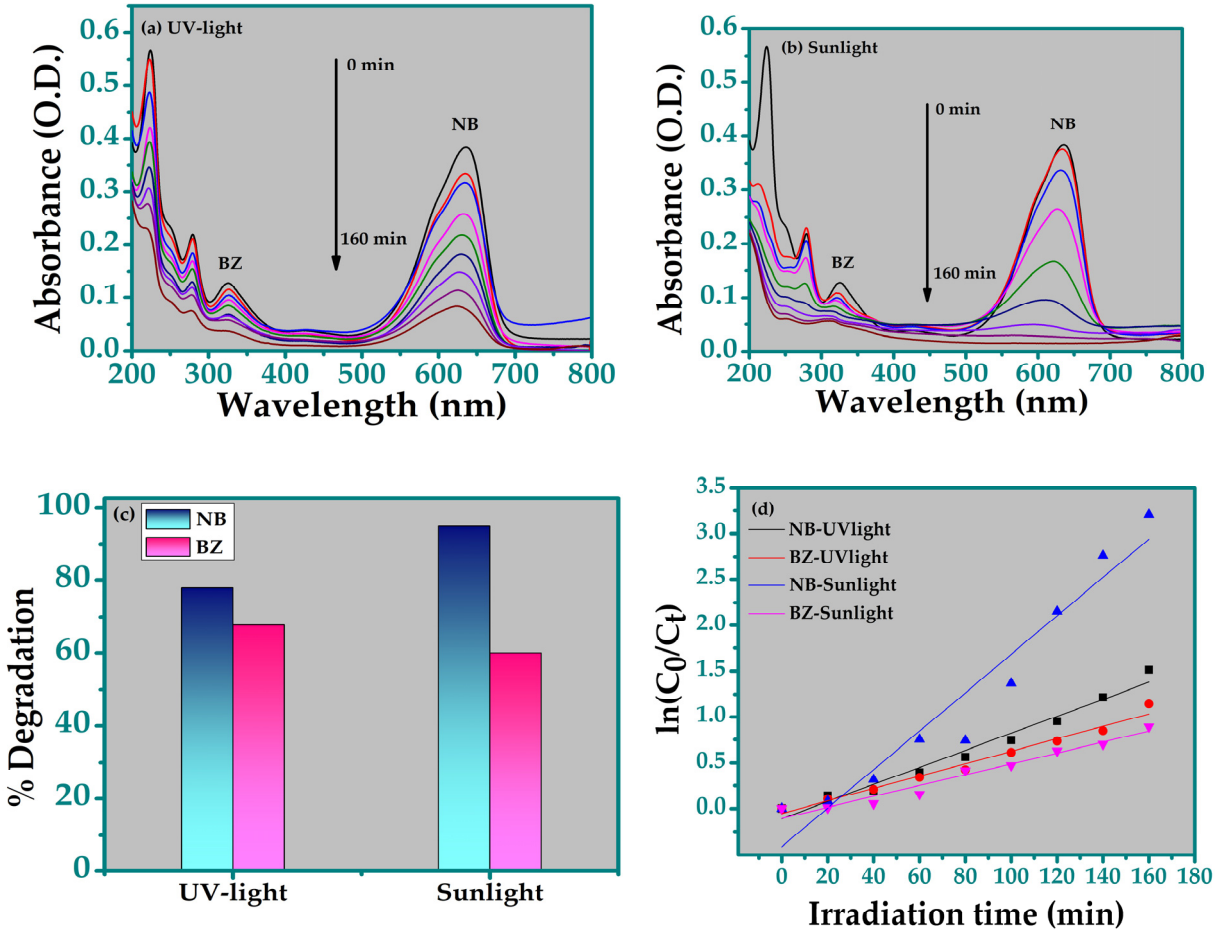

Figure 7. Absorption spectra of BZ + NB solution in the presence of TiO_2 photocatalyst under UV (**a**) and sunlight (**b**); degradation efficiency at different time intervals for TiO_2 photocatalyst (**c**); degradation rate constant plots for NB and BZ in the mixture (**d**).

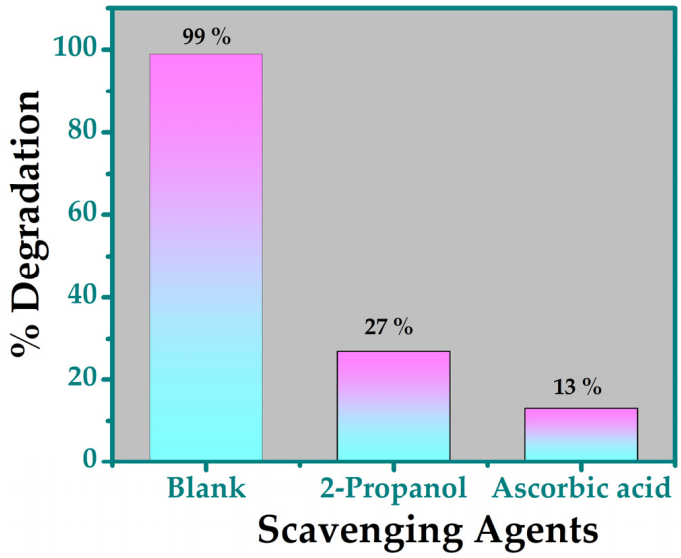

Figure 8. Effect of scavengers on the degradation efficiency of bentazon under UV light.

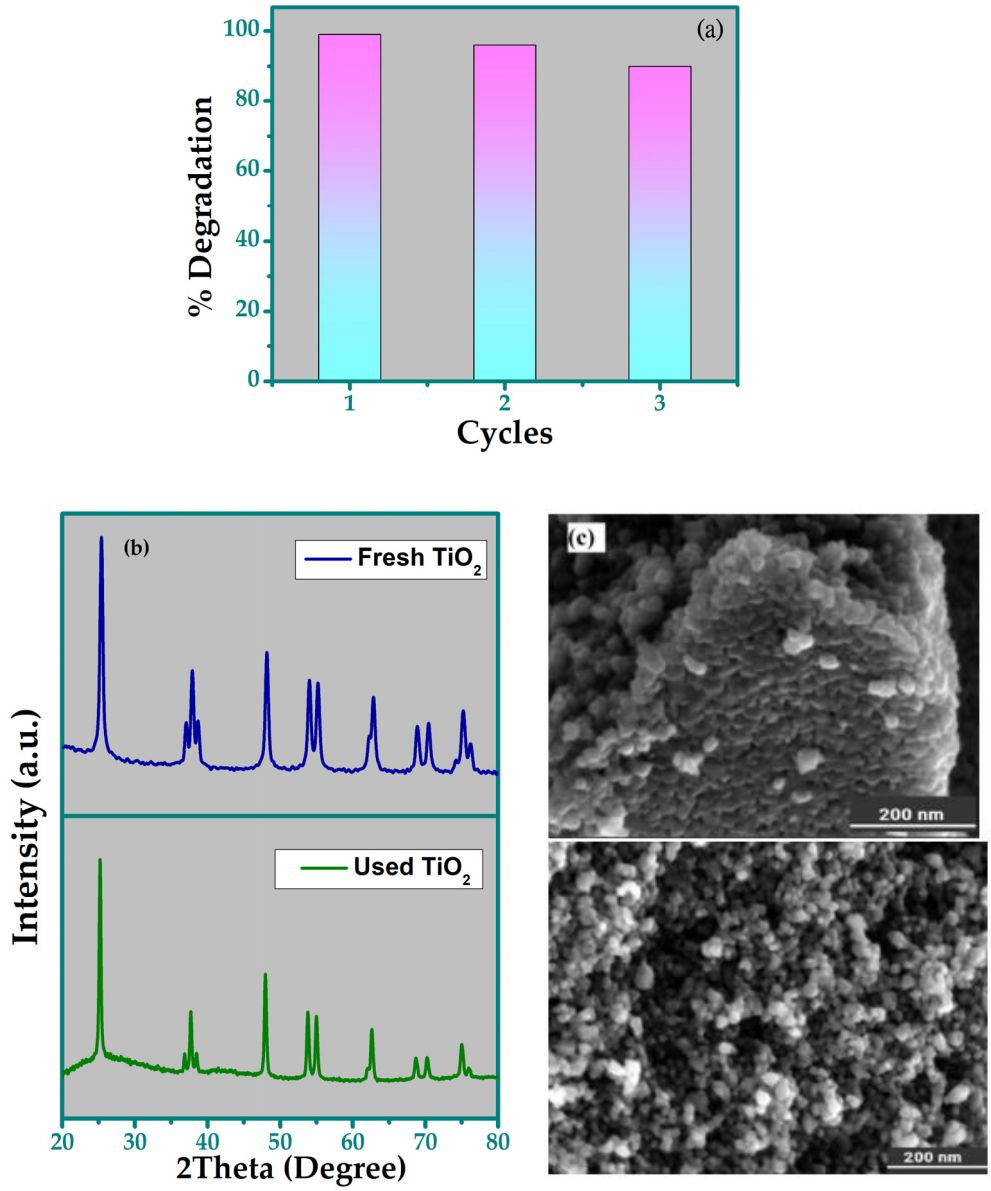

Figure 9. (**a**) reusability test for three cycles, (**b**) XRD of fresh and reused TiO_2 photocatalyst for three cycles, (**c**) SEM images of fresh and reused TiO_2 photocatalyst.

4. Conclusions

TiO_2 nanoparticles were prepared using $TiCl_4$ as a precursor via sol–gel synthesis. The prepared TiO_2 photocatalyst was used for the degradation of BZ herbicide and NB dye and their mixture under UV and sunlight. The TiO_2 catalyst completely degraded both pollutants under UV light and the efficiency was 99% and 98% for BZ and NB, respectively. The obtained degradation efficiency under sunlight was 75% and 100% for BZ and NB, respectively. For the BZ + NB mixture, both pollutants degrade simultaneously under UV and sunlight. However, the degradation rate for BZ was lower as compared to NB under both light sources, which indicates that due to its complex structure, NB affects the degradation rate of BZ. The obtained results indicate that the TiO_2 photocatalyst is a potential candidate for the photodegradation of dyes and herbicides and their mixture solutions under UV and sunlight.

Author Contributions: Conceptualization, S.Y. and L.B.; methodology, S.Y., L.B. and P.P.; validation, L.B., P.P. and L.D.; formal analysis, S.Y.; investigation, S.Y., L.B., L.D., E.S. and A.A.; data curation, S.Y. and L.B.; writing—original draft preparation, S.Y.; writing—review and editing, P.P., L.B., L.D., E.S. and A.A.; supervision, P.P. All the authors have read and agreed to the published version of the manuscript. All authors have read and agreed to the published version of the manuscript.

Funding: This research received no external funding.

Institutional Review Board Statement: Not applicable.

Informed Consent Statement: Not applicable.

Data Availability Statement: The original contributions presented in the study are included in the article, further inquiries can be directed to the corresponding author.

Conflicts of Interest: The authors declare no conflicts of interest.

References

1. Tölgyesi, Á.; Korozs, G.; Tóth, E.; Bálint, M.; Ma, X.; Sharma, V.K. Automation in Quantifying Phenoxy Herbicides and Bentazon in Surface Water and Groundwater Using Novel Solid Phase Extraction and Liquid Chromatography Tandem Mass Spectrometry. *Chemosphere* **2022**, *286*, 131927. [CrossRef] [PubMed]
2. Guelfi, D.R.V.; Brillas, E.; Gozzi, F.; Machulek, A.; de Oliveira, S.C.; Sirés, I. Influence of Electrolysis Conditions on the Treatment of Herbicide Bentazon Using Artificial UVA Radiation and Sunlight. Identification of Oxidation Products. *J. Environ. Manag.* **2019**, *231*, 213–221. [CrossRef] [PubMed]
3. Negash, A.; Mohammed, S.; Weldekirstos, H.D.; Ambaye, A.D.; Gashu, M. Enhanced Photocatalytic Degradation of Methylene Blue Dye Using Eco-Friendly Synthesized RGO@ZnO Nanocomposites. *Sci. Rep.* **2023**, *13*, 22234. [CrossRef] [PubMed]
4. Olas, B.; Białecki, J.; Urbańska, K.; Bryś, M. The Effects of Natural and Synthetic Blue Dyes on Human Health: A Review of Current Knowledge and Therapeutic Perspectives. *Adv. Nutr.* **2021**, *12*, 2301–2311. [CrossRef] [PubMed]
5. Rashid, R.; Shafiq, I.; Akhter, P.; Iqbal, M.J.; Hussain, M. A State-of-the-Art Review on Wastewater Treatment Techniques: The Effectiveness of Adsorption Method. *Environ. Sci. Pollut. Res.* **2021**, *28*, 9050–9066. [CrossRef]
6. Al-Mamun, M.R.; Kader, S.; Islam, M.S.; Khan, M.Z.H. Photocatalytic Activity Improvement and Application of UV-TiO_2 Photocatalysis in Textile Wastewater Treatment: A Review. *J. Environ. Chem. Eng.* **2019**, *7*, 103248. [CrossRef]
7. Hitam, C.N.C.; Jalil, A.A. A Review on Exploration of Fe_2O_3 Photocatalyst towards Degradation of Dyes and Organic Contaminants. *J. Environ. Manag.* **2020**, *258*, 110050. [CrossRef]
8. Ferreira, S.H.; Morais, M.; Nunes, D.; Oliveira, M.J.; Rovisco, A.; Pimentel, A.; Águas, H.; Fortunato, E.; Martins, R. High UV and Sunlight Photocatalytic Performance of Porous ZnO Nanostructures Synthesized by a Facile and Fast Microwave Hydrothermal Method. *Materials* **2021**, *14*, 2385. [CrossRef] [PubMed]
9. Sakthivel, S.; Hidalgo, M.C.; Bahnemann, D.W.; Geissen, S.U.; Murugesan, V.; Vogelpohl, A. A Fine Route to Tune the Photocatalytic Activity of TiO_2. *Appl. Catal. B Environ.* **2006**, *63*, 31–40. [CrossRef]
10. Zarubica, A.; Ljupković, R.; Papan, J.; Vukoje, I.; Porobić, S.; Ahrenkiel, S.P.; Nedeljković, J.M. Visible-Light-Responsive Al_2O_3 Powder: Photocatalytic Study. *Opt. Mater.* **2020**, *106*, 110013. [CrossRef]
11. Krishnan, S.; Shriwastav, A. Application of TiO_2 Nanoparticles Sensitized with Natural Chlorophyll Pigments as Catalyst for Visible Light Photocatalytic Degradation of Methylene Blue. *J. Environ. Chem. Eng.* **2021**, *9*, 104699. [CrossRef]
12. Verma, V.; Al-Dossari, M.; Singh, J.; Rawat, M.; Kordy, M.G.M.; Shaban, M. A Review on Green Synthesis of TiO_2 NPs: Synthesis and Applications in Photocatalysis and Antimicrobial. *Polymers* **2022**, *14*, 1444. [CrossRef]
13. Banerjee, A.N.; Hamnabard, N.; Joo, S.W. A Comparative Study of the Effect of Pd-Doping on the Structural, Optical, and Photocatalytic Properties of Sol–Gel Derived Anatase TiO_2 Nanoparticles. *Ceram. Int.* **2016**, *42*, 12010–12026. [CrossRef]
14. Rueda-Marquez, J.J.; Levchuk, I.; Fernández Ibañez, P.; Sillanpää, M. A Critical Review on Application of Photocatalysis for Toxicity Reduction of Real Wastewaters. *J. Clean. Prod.* **2020**, *258*, 120694. [CrossRef]
15. Racovita, A.D. Titanium Dioxide: Structure, Impact, and Toxicity. *Int. J. Environ. Res. Public Health* **2022**, *19*, 5681. [CrossRef] [PubMed]
16. Li, W.; Zeng, T. Preparation of TiO_2 Anatase Nanocrystals by $TiCl_4$ Hydrolysis with Additive H_2SO_4. *PLoS ONE* **2011**, *6*, e21082. [CrossRef]
17. Lee, D.S.; Liu, T.K. Preparation of TiO_2 Sol Using $TiCl_4$ as a Precursor. *J. Sol-Gel Sci. Technol.* **2002**, *25*, 121–136. [CrossRef]
18. Wang, Z.; Liu, S.; Cao, X.; Wu, S.; Liu, C.; Li, G.; Jiang, W.; Wang, H.; Wang, N.; Ding, W. Preparation and Characterization of TiO_2 Nanoparticles by Two Different Precipitation Methods. *Ceram. Int.* **2020**, *46*, 15333–15341. [CrossRef]

19. Elsellami, L.; Dappozze, F.; Fessi, N.; Houas, A.; Guillard, C. Highly Photocatalytic Activity of Nanocrystalline TiO_2 (Anatase, Rutile) Powders Prepared from $TiCl_4$ by Sol–Gel Method in Aqueous Solutions. *Process Saf. Environ. Prot.* **2018**, *113*, 109–121. [CrossRef]
20. Subhan, M.A.; Uddin, N.; Sarker, P.; Azad, A.K.; Begum, K. Photoluminescence, Photocatalytic and Antibacterial Activities of CeO_2·CuO·ZnO Nanocomposite Fabricated by Co-Precipitation Method. *Spectrochim. Acta Part A Mol. Biomol. Spectrosc.* **2015**, *149*, 839–850. [CrossRef] [PubMed]
21. Rajeev, Y.N.; Magdalane, C.M.; Ramalingam, G.; Kumar, L.B.; Alwadai, N.; Al-Buriahi, M.S. Photocatalytic Activity of Hierarchical CTAB-Assisted TiO_2 Nanoparticles for Polluted Water Treatment Using Solar Light Illumination. *Appl. Phys. A* **2022**, *128*, 299. [CrossRef]
22. Suresh, R.; Ponnuswamy, V.; Mariappan, R. Effect of Annealing Temperature on the Microstructural, Optical and Electrical Properties of CeO_2 Nanoparticles by Chemical Precipitation Method. *Appl. Surf. Sci.* **2013**, *273*, 457–464. [CrossRef]
23. Ahmad, M.M.; Mushtaq, S.; Al Qahtani, H.S.; Sedky, A.; Alam, M.W. Investigation of Tio_2 Nanoparticles Synthesized by Sol-Gel Method for Effectual Photodegradation, Oxidation and Reduction Reaction. *Crystals* **2021**, *11*, 1456. [CrossRef]
24. Gholami, M.; Jonidi-Jafari, A.; Farzadkia, M.; Esrafili, A.; Godini, K.; Shirzad-Siboni, M. Photocatalytic Removal of Bentazon by Copper Doped Zinc Oxide Nanorods: Reaction Pathways and Toxicity Studies. *J. Environ. Manag.* **2021**, *294*, 112962. [CrossRef]
25. Haque, F.Z.; Nandanwar, R.; Singh, P. Evaluating Photodegradation Properties of Anatase and Rutile TiO_2 Nanoparticles for Organic Compounds. *Optik* **2017**, *128*, 191–200. [CrossRef]
26. John, A.K.; Palaty, S.; Sharma, S.S. Greener Approach towards the Synthesis of Titanium Dioxide Nanostructures with Exposed {001} Facets for Enhanced Visible Light Photodegradation of Organic Pollutants. *J. Mater. Sci. Mater. Electron.* **2020**, *31*, 20868–20882. [CrossRef]
27. Zainab, S.; Azeem, M.; Awan, S.U.; Rizwan, S.; Iqbal, N.; Rashid, J. Optimization of Bandgap Reduction in 2-Dimensional GO Nanosheets and Nanocomposites of GO/Iron-Oxide for Electronic Device Applications. *Sci. Rep.* **2023**, *13*, 1–19. [CrossRef]
28. Rabia, M.; Mohamed, S.H.; Zhao, H.; Shaban, M.; Lei, Y.; Ahmed, A.M. TiO_2/TiOxNY Hollow Mushrooms-like Nanocomposite Photoanode for Hydrogen Electrogeneration. *J. Porous Mater.* **2020**, *27*, 133–139. [CrossRef]
29. Yasmeen, S.; Burratti, L.; Duranti, L.; Agresti, A. Study of Photodegradation of Bentazon Herbicide by Using ZnO-Sm_2O_3 Nanocomposite Under UV Light. *Int. J. Mol.Sci.* **2024**, *25*, 13319. [CrossRef]
30. Seck, E.I.; Doña-Rodríguez, J.M.; Fernández-Rodríguez, C.; Portillo-Carrizo, D.; Hernández-Rodríguez, M.J.; González-Díaz, O.M.; Pérez-Peña, J. Solar Photocatalytic Removal of Herbicides from Real Water by Using Sol-Gel Synthesized Nanocrystalline TiO_2: Operational Parameters Optimization and Toxicity Studies. *Sol. Energy* **2013**, *87*, 150–157. [CrossRef]
31. Kinkennon, A.E.; Green, D.B.; Hutchinson, B. The Use of Simulated or Concentrated Natural Solar Radiation for the TiO_2-Mediated Photodecomposition of Basagran, Diquat, and Diuron. *Chemosphere* **1995**, *31*, 8663–8671. [CrossRef]
32. Ahmed, S. Preparation and Characterization of ZnO & TiO_2 Nanocatalysts for Photo Degradation of Bentazon Existing in Polluted Water. *J. Phys. Conf. Ser.* **2019**, *1310*, 012015. [CrossRef]
33. Mungondori, H.H.; Tichagwa, L.; Katwire, D.M.; Aoyi, O. Preparation of Photo-Catalytic Copolymer Grafted Asymmetric Membranes (N-TiO_2-PMAA-g-PVDF/PAN) and Their Application on the Degradation of Bentazon in Water. *Iran. Polym. J.* **2016**, *25*, 135–144. [CrossRef]
34. Yaseen, M.; Humayun, M.; Khan, A.; Idrees, M.; Shah, N.; Bibi, S. Photo-Assisted Removal of Rhodamine B and Nile Blue Dyes from Water Using CuO–SiO_2 Composite. *Molecules* **2022**, *27*, 5343. [CrossRef] [PubMed]
35. Habibi, M.H.; Mosavi, V. Wet Coprecipitation Preparation of Perovskite-Type Iron Manganite Nano Powder Pure Phase Using Nitrate Precursors: Structural, Opto-Electronic, Morphological and Photocatalytic Activity for Degradation of Nile Blue Dye. *J. Mater. Sci. Mater. Electron.* **2017**, *28*, 10270–10276. [CrossRef]
36. Mirzaei, M.; Habibi, M.H.; Sabzyan, H. Synthesis, Characterization, and Dye Degradation Photocatalytic Activity of the Nano-Size Copper Iron Binary Oxide. *Environ. Sci. Pollut. Res.* **2022**, *29*, 9173–9192. [CrossRef] [PubMed]
37. Yasmeen, S.; Burratti, L.; Duranti, L.; Sgreccia, E.; Prosposito, P. Photocatalytic Degradation of Organic Pollutants—Nile Blue, Methylene Blue, and Bentazon Herbicide—Using NiO-ZnO Nanocomposite. *Nanomaterials* **2024**, *14*, 470. [CrossRef] [PubMed]
38. Prabhudesai, V.S.; Meshram, A.A.; Vinu, R.; Sontakke, S.M. Superior Photocatalytic Removal of Metamitron and Its Mixture with Rhodamine B Dye Using Combustion Synthesized TiO_2 Nanomaterial. *Chem. Eng. J. Adv.* **2021**, *5*, 100084. [CrossRef]
39. Sabzehmeidani, M.M.; Karimi, H.; Ghaedi, M. Degradation of Binary Mixtures of Dyes by Step-Scheme Quaternary Photocatalyst in Continuous Flow-Loop Ultrasound Assisted Micro-Photoreactor. *J. Mol. Liq.* **2023**, *388*, 122830. [CrossRef]